

# Side wall effects of ship model tests in shallow water waves

Manases Tello Ruiz<sup>1\*</sup>, Wim Van Hoydonck<sup>2</sup>, Guillaume Delefortrie<sup>2</sup>, and Marc Vantorre<sup>1</sup>

<sup>1</sup>Ghent University, Technologiepark Zwijnaarde 904, Ghent 9052, Belgium

<sup>2</sup>Flanders Hydraulics Research, Berchemlei 115, Antwerp 2140, Belgium

\*manases.ruiz @ugent.be

## 1 Introduction

Ship model tests in waves are limited to specific combination of model speeds, main wave parameters, and the tank's main dimensions. Side wall effects are major constraints to tests in waves and their effects can be relatively significant (Kashiwagi et al., 1990, Chen, 1994, and Zhu et al., 2011). For tests at zero forward speed, according to Chen (1994), side wall effects are important for both the first and second order quantities. Similar results were found by Zhu et al. (2011) for an open ship in oblique seas. Kashiwagi et al. (1990) studied the non-zero forward speed case for deep water and concluded that, although side wall effects occur, a limiting region where the side wall effects are less than 10% of the quantities obtained in open sea can be determined.

The ITTC–Recommended Procedures and Guidelines, Seakeeping experiments (7.5-02 07-02.1) provides practical guidelines to select test parameters at which side wall effects are avoided. This is obtained by simply selecting ship speeds higher than a critical speed  $Fr_{crit}$ . This critical speed (assuming the ship is moving on a straight course along the centre line of the tank ) results from the time needed for the radiated waves to travel back and forth and the time needed for the ship to move one ship length (see LLoyd, 1989, and ITTC, 2014).

The ITTC speed limits are a function of the tank's width  $W_T$  to ship length  $L_{PP}$  ratio  $r = W_T/L_{PP}$ , independently of the waves. This general relationship is possible because deep water is assumed. As wave characteristics depend on the water depth this relationship is not valid for finite water depths. Hence, the speed limits for finite water depths must be estimated including the wave characteristics.

In finite water depths, shallow water from the ship's point of view ( $1.5 > h.T_m > 1.2$ , PIANC, 2012), the ITTC guidelines are very restrictive, because the required speeds to avoid side wall effects do not necessarily comply with the common practice of low to moderate manoeuvring speeds. The available range of test parameters is then reduced to a few possible combinations of waves and ship speeds. An obvious solution is to use a wider tank; this is, however, an expensive solution, not only from the experimental point of view but also from computational requirements if CFD methods are used.

To investigate a possible solution to increase the suitability of model tests in shallow water waves, experimental and numerical studies have been conducted at Flanders Hydraulics Research (FHR) in Antwerp, Belgium (in cooperation with Ghent University). The study includes experimental and numerical results obtained from two container ship models, the KCS and a scale model of an ULCS (referred to as COW). Model tests included different ship speeds, wave frequencies, and offsets from the tank's centre line. The numerical study was carried out for two different tank widths with the CFD software package FINE<sup>TM</sup>/Marine.

## 2 Experimental and computational program

### 2.1 Experimental set-up

The experiments were conducted at the Towing Tank for Manoeuvres in Shallow Water at Flanders Hydraulics Research (FHR) in Antwerp, Belgium (in cooperation with Ghent University). Delefortrie et al. (2016) presented the towing tank's main characteristics. During tests horizontal forces were measured by the load cells LC1 and LC2 and the ship's heave and pitch were obtained by using four potentiometers P1 to P4 (see Figure 1a,b). Wave profiles were recorded with four wave gauges: WG1 to WG3 were located at a fixed position along the tank and WG4 was attached to the main carriage (see Figure 1c). Positions and orientations during tests are defined by using two coordinate systems,

an Earth-fixed coordinate system  $O_0x_0y_0z_0$  and a body-fixed coordinate system  $Oxyz$ , both North-East-Down oriented, see Figure 1c.

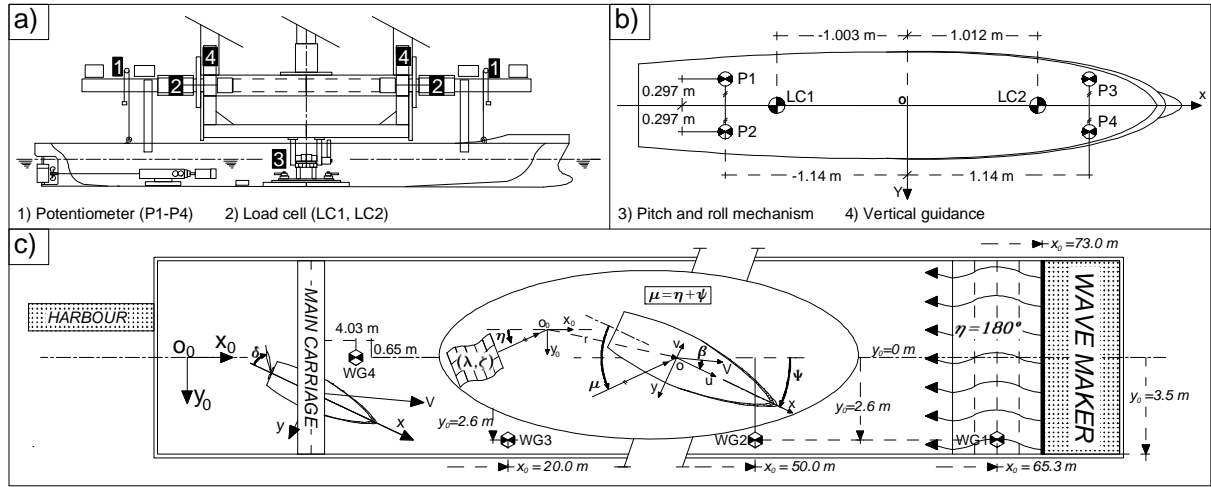


Figure 1 Towing tank at FHR, set-up for semi captive tests for both the COW and the KCS ship.

The ship models main parameters for the KCS and the COW are given in Table 1.

Table 1 Container ship models main parameters.

Ship	$L_{pp}(m)$	$B(m)$	$T_m(m)$	$C_b$	$\nabla(m^3)$	$x_G(m)$	$z_G(m)$	$r_{44}(m)$	$r_{55}(m)$	$r_{66}(m)$
KCS	4.367	0.611	0.205	0.651	0.356	-0.07	-0.03	0.20	1.07	1.09
COW	4.191	0.627	0.161	0.594	0.258	-0.114	0.00	0.22	1.03	1.05

## 2.2 Computational set-up

### Domain

The wide case domain length ( $x$ -direction) is  $8 L_{pp}$ :  $2 L_{pp}$  between the ship's bow and the inlet boundary and  $5 L_{pp}$  between the ship's transom and the aft (outlet) boundary. The width of the domain is approximately  $2 L_{pp}$ . The narrow case has the same longitudinal dimensions as the wide case, its width is equal to half the width of the towing tank of FHR (3.5 m). For both condition the ship's ukc set to 50% and height of the domains are set to equals the water level plus  $1 L_{pp}$ .

### Grid

To ensure that the wave shape remains constant between the inlet and the ship, the grid near the still water level is refined with a refinement box (box 1 in Figure 2), both in the wave height ( $H$ ) and wavelength directions ( $\lambda$ ) by the discretization:  $dx = \lambda/60$ ,  $dz = H/16$ . The target cell size in the  $x$ -direction and the  $y$ -direction are the same. Numerical damping of the wave aft of the vessel is achieved by a three-step coarsening of the cells in the  $x$ - and  $y$ -direction (see box 2 to box 4 in Figure 2) starting at  $1 L_{pp}$  aft of the vessel (in the  $z$ -direction, the cell size is kept constant). In each step, the linear dimensions are doubled.

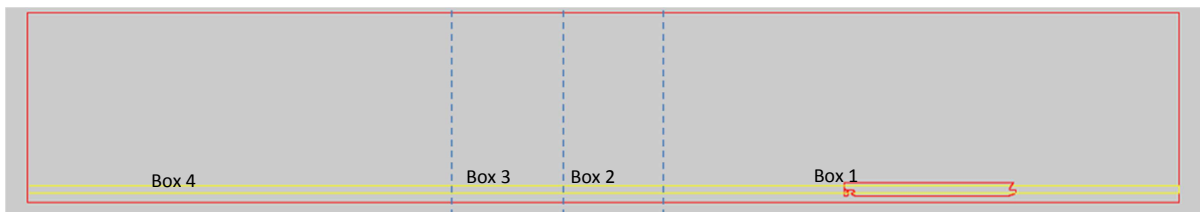


Figure 2 Mesh refinement boxes to ensure a constant wave shape (box1), and incorporate numerical damping (box 2, box 3, box 4).

To resolve the boundary layer that develops due to viscosity, a high-quality viscous layer is inserted around the hull. Wall functions are used on the complete hull except for the deck, where a slip boundary condition is applied. The target  $y^+$  value was set to 30. With a reference velocity of 1.0398 m/s (relative velocity between ship and wave) and a reference length of 2.0955 m (wavelength), the first layer height becomes 1.132 mm. Total mesh size after inserting the viscous layers is  $13.4 \cdot 10^6$  cells for the case with the wide tank. For the narrow tank case, the cell count is approximately  $6 \cdot 10^6$ .

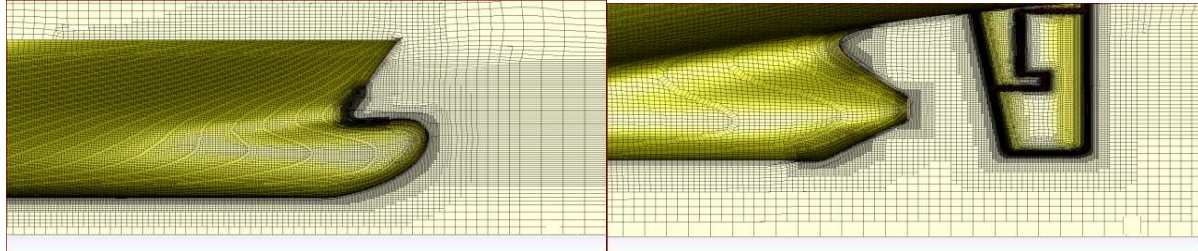


Figure 3 Mesh refinement on the hull surface at the bow (left) and the stern (right).

### Boundary Conditions

For the complete ship and rudder wall functions are assumed, except for the deck, where a slip (zero shear stress) boundary condition is applied. For the bottom of the tank, a slip boundary condition is used as well. At the domain top, the pressure is prescribed based on the hydrostatic pressure. For the outlet, a far field condition is used for the velocity ( $V = 0$  m/s). At the inlet, a wave generator boundary condition is employed that generates regular third-order Stokes waves. For the lateral side, a zero-pressure gradient boundary condition is applied.

### Solver settings

The computation is started with the vessel at rest. During the first 8 seconds, the speed of the vessel is smoothly increased to 0.542 m/s. Heave and pitch of the vessel are solved, the other degrees of freedom are held fixed. Each time step, the solver executes a maximum of 20 non-linear iterations. By default, 23200 time steps with a step size of 0.0067 s are executed (~155 seconds).

### 2.3 Test matrix

The main parameters for the experimental and numerical analysis are presented in Table 2. Wave lengths of regular waves RW are given as a function of the ship length  $L_{PP}$ , with wave heights (trough to crest) of 0.04 m and 0.08 m for the COW and the KCS, respectively. Ship speeds ( $Fr_h$ ) as a Froude to depth number, and the tank's width  $W_T$  to ship length  $L_{PP}$  ratio  $r = W_T/L_{PP}$  are calculated for each ship. The test matrix leads to sixteen EFD tests for the KCS ship and to two CFD tests for the COW. The water depths  $h$  correspond to 100% and 50% ukc for the KCS and the COW, respectively.

Table 2 Experimental and numerical parameters for model test in waves.

KCS ship, EFD, $h = 0.410$ (m)								COW ship, CFD, $h = 0.242$ (m)			
$W_T/L_{PP}$				Speeds		Waves		$W_T/L_{PP}$		Speeds	Waves
$r1$	$r2$	$r3$	$r4$	$Fr_{h1}$	$Fr_{h2}$	$RW_1$	$RW_2$	$r1$	$r2$	$Fr_{h1}$	$RW_1$
1.60	1.51	1.37	1.15	0.124	0.424	$0.4L_{PP}$	$0.6L_{PP}$	1.67	3.97	0.352	$0.45L_{PP}$

The sixteen different EFD tests with the KCS were obtained by running the same speed and wave length at four different offsets from the tank's centre line, while the two numerical simulations for the COW were conducted with CFD with two different tank widths.

### 3 Experimental analysis and discussions

The critical speeds (based on the ITTC guidelines) obtained with the KCS for the four  $r$  ratios are plotted in Figure 4 with continuous lines, while the 16 EFD tests are displayed with square markers. The ratios between the critical speed and the speeds used during tests are given in Table 3.

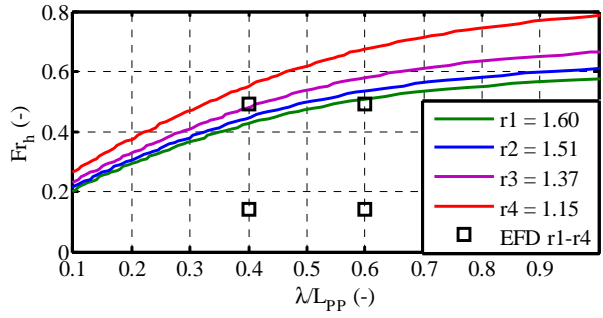


Table 3 KCS ship speed to critical speed ratios.

Speed (-)	$W_T/L_{PP}$ (-)				$\lambda$ (-)
	$r_1$	$r_2$	$r_3$	$r_4$	
$Fr_{h1}/Fr_{hcrit}$	0.33	0.32	0.29	0.26	$0.4L_{PP}$
$Fr_{h2}/Fr_{hcrit}$	0.27	0.25	0.24	0.20	$0.6L_{PP}$
$Fr_{h1}/Fr_{hcrit}$	1.17	1.11	1.03	0.91	$0.4L_{PP}$
$Fr_{h2}/Fr_{hcrit}$	0.94	0.90	0.83	0.72	$0.6L_{PP}$

Figure 4 Critical speeds for the KCS ship.

From Figure 4, all tests seem to suffer from side wall interaction (following ITTC guidelines) with the exception of tests at  $Fr_{h2}, 0.4L_{PP}$ , and ratios  $r_1$  to  $r_3$  (see Table 3, where  $Fr_{h2}/Fr_{hcrit} > 1$ ). Then, tests at lower  $Fr_{h2}/Fr_{hcrit}$  would be principally excluded from the study. To evaluate if side wall effects are present/significant, a Fourier analysis was conducted for all tests. The results are shown together for the same speed and wave length but for the four different ratios  $r$  in Figure 5. Results obtained for  $0.4L_{PP}$  and  $0.6L_{PP}$  are plotted in the first/second and the third/fourth row, respectively.

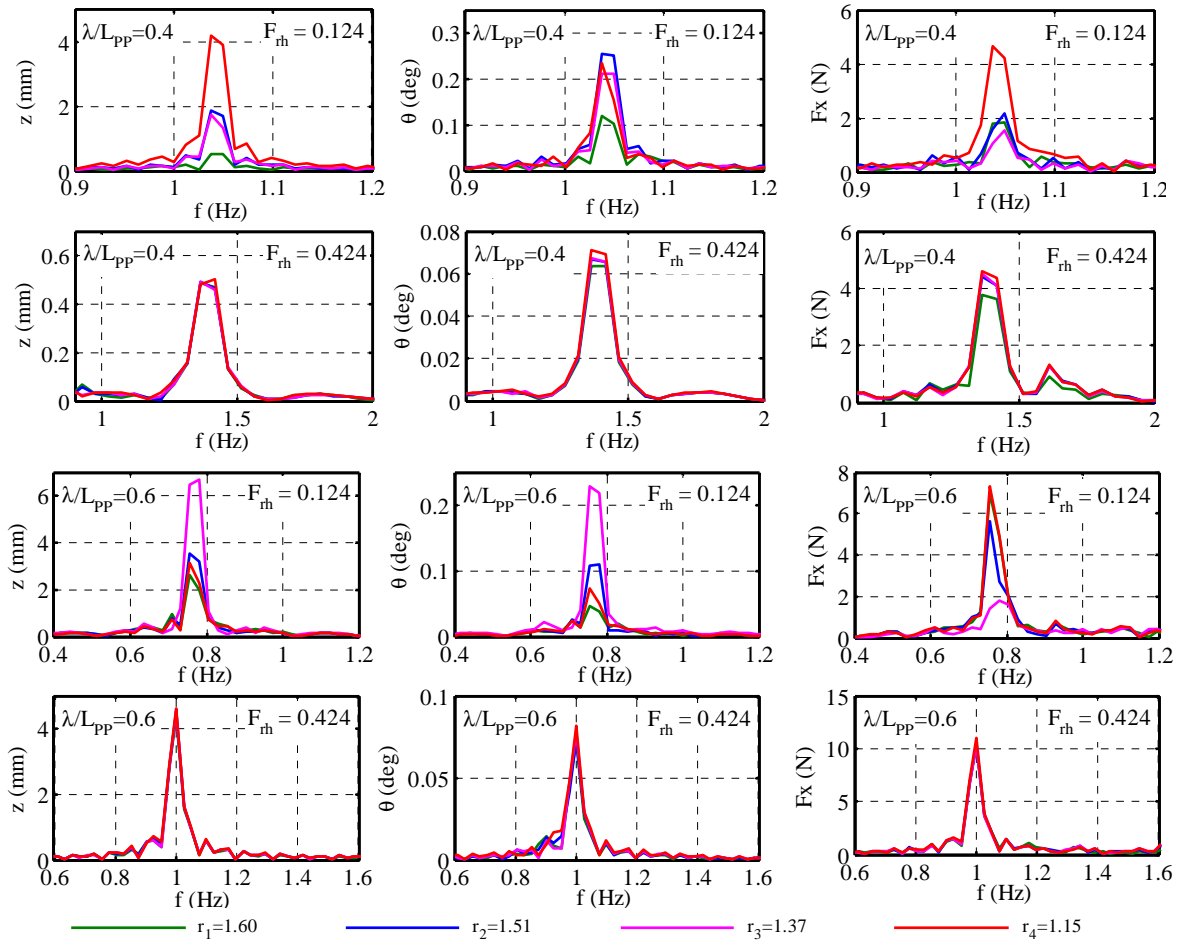


Figure 5 Spectral analysis of the KCS test in waves for four different  $r$  ratios.

From Figure 5, significant side wall influence is observed for results obtained at low ship speed to critical speed ratios,  $Fr_h/Fr_{hcrit} < 0.35$  (first and third row in Figure 5, see Table 3). In contrast, for tests at  $Fr_h/Fr_{hcrit} > 0.70$  results remain the same, thus indicating negligible side wall effects. This seems to introduce a new limit to define whether tests, expected to suffer from side wall interaction, can yet be performed.

## 4 Numerical analysis and discussions

To verify the observed speed limit  $Fr_h/Fr_{hcrit} > 0.70$ , a CFD study was carried out for the COW ship model with two different tank's width, see Table 2. The ship was set free to heave and pitch. For both tests, the same wave length, ship speed, and water depth were used. The CFD study was conducted with the software package FINE<sup>TM</sup>/Marine.

The corresponding speed limits for these two cases and the numerical solutions are plotted in Figure 6. The respective means ( $a_0$ ), height ( $H$ , trough to crest) and periods ( $T$ ) of the harmonic signals are given in Table 4.

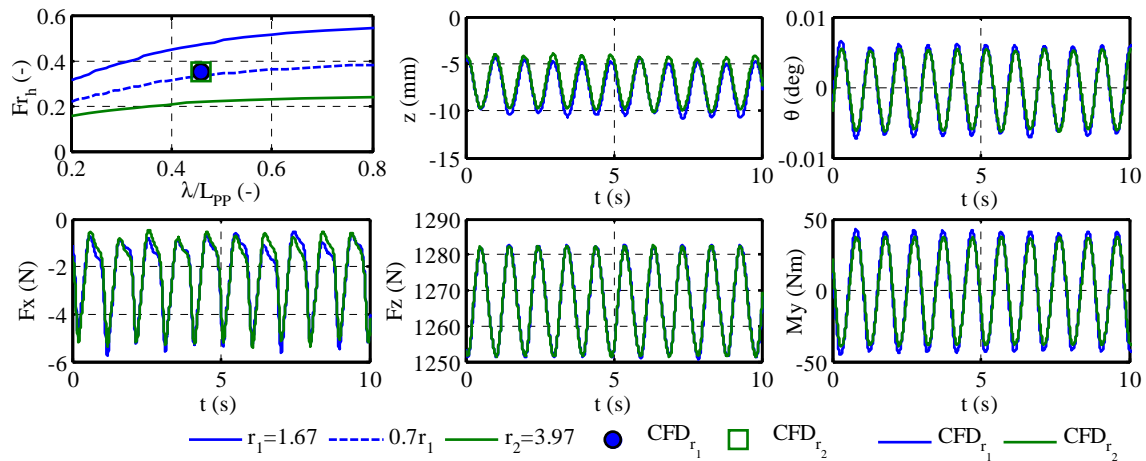


Figure 6 COW ship model, (top-left) critical speeds, and motion responses from the two CFD studies.

Table 4 Mean and harmonic components of the two CFD computations.

Items	$z$ (mm)		$\theta$ (deg)		$F_x$ (N)		$F_z$ (N)		$M_y$ (Nm)	
	r1	r2	r1	r2	r1	r2	r1	r2	r1	r2
$a_0$	-6.76	-6.25	0.00	0.00	-2.25	-2.19	1267.08	1267.07	0.00	0.01
$H$	5.78	5.69	0.01	0.01	4.42	4.46	31.55	30.90	83.97	76.08
$T$ (s)	0.16	0.16	0.16	0.16	0.16	0.16	0.16	0.16	0.16	0.16

From Figure 6 and Table 4, the ship's responses, forces and motions, do not show any significant variation between the narrower and wider tank. The largest influence is even less than 8%, obtained for the sinkage ( $a_0$ , corresponding to  $z$ ). Thus the signals appear to not suffer significantly from side wall effects. Although the results are obtained for another ship and a different test configuration, this seems to confirm the limits observed with the EFD tests for the KCS ship.

## 5 Conclusion

The study shows that side wall interaction does not influence significantly ship model tests in waves for ship speeds higher than 70% of the critical speed (determined based on the ITTC approach expressed in shallow water conditions). Although this is not yet confirmed for other ship types, the reduction of the speed limits seems considerably important. This does not only represent an advantage for experimental analysis only, but also for numerical studies in which reducing the width of the numerical domain would decrease significantly computational time.

## Acknowledgements

The present work was performed in the frame of project WL\_2013\_47 (Scientific support for investigating the manoeuvring behaviour of ships in waves), granted to Ghent University by Flanders Hydraulics Research, Antwerp (Department of Mobility and Public Works, Flemish Government, Belgium). For the numerical studies the authors would like to thank NUMECA for the cooperation, which is highly appreciated.

## References

- X. Chen (1994). On the side wall effects upon bodies of arbitrary geometry in wave tanks. *Applied Ocean Research*, 16(6), 337–345.
- G. Delefortrie, S. Geerts, and M. Vantorre (2016). The towing tank for manoeuvres in shallow water. MASHCON 2016. Hamburg, Germany.
- ITTC (2014). ITTC – Recommended procedures and guidelines. Seakeeping experiments (7.5-02 07-02.1).
- M. Kashiwagi, M. Ohkusu, and M. Inada, M. (1990). Side-Wall Effects on Radiation and Diffraction Forces on a Ship Advancing in Waves. *Journal of The Society of Naval Architects of Japan*, 1990(168), 227–242.
- A.R.J.M. LLoyd (1989). *Seakeeping: ship behaviour in rough weather*. (Ellis Horwood, Ed.). Ellis Horwood Series in Marine technology.
- S. Zhu, M. Wu, and T. Moan, T. (2011). Experimental and Numerical Study of Wave-Induced Load Effects of Open Ships in Oblique Seas. *Journal of Ship Research*, 55(24), 100–123.